Spin-lattice coupling and phonon dispersion of CdCr_{2}O_{4} from first principles

A. Kumar, C. J. Fennie, and K. M. Rabe

Spin-lattice coupling and phonon dispersion of CdCr$_2$O$_4$ from first principles

A. Kumar[1], C. J. Fennie[2] and K. M. Rabe[1]

[1]*Department of Physics and Astronomy, Rutgers University, Piscataway, New Jersey 08854, USA*

[2]*School of Applied and Engineering Physics, Cornell University, Ithaca, New York 14853, USA*

(Dated: November 16, 2012)

First principles calculations are used to investigate the effects of magnetic ordering on the minimum-energy structure and on the full phonon dispersion relation of CdCr$_2$O$_4$, focusing on the changes through the coupled magnetic/structural transition which shows relief of the geometric frustration of the antiferromagnetic ordering on the pyrochlore lattice. We computed the full phonon dispersion relations for the ferromagnetic and antiferromagnetic orderings in cubic and tetragonal structures of CdCr$_2$O$_4$. We extracted the phonon dispersion for the cubic paramagnetic phase and found that it compares well with the experimental results. The AFM ordering is seen to lower the symmetry and induce a lattice distortion comparable in magnitude to that observed in the transition. While the spin-phonon couplings are large for modes which involve displacement of the Cr atoms, there are no unstable modes at any point in the Brillouin zone for either of the magnetic orderings considered, and thus we conclude that the phase transition is driven not by spin-phonon coupling, but by the atomic forces and stresses induced by the magnetic order. Finally, by comparison of the phonon frequencies for structures with different magnetic orderings and structural distortions, we find that the spin-phonon coupling, rather than the coupling of the phonons to the structural change, is the dominant factor in the observed changes of phonon frequencies through the phase transition.

I. INTRODUCTION

The physics of frustrated magnetism is a subject of continuing interest[1,2]. Spinel oxides AB$_2$O$_4$ with magnetic B cations have received particular attention because they are characterized by three-dimensional geometrical frustration[3–8]. The spinel structure is cubic ($Fd\bar{3}m$ No. 227) with the A cation tetrahedrally coordinated by oxygens and the B cation octahedrally coordinated by oxygens (see Figure 1). The octahedral sites occupied by B magnetic ions form a pyrochlore lattice, which is a three-dimensional network of corner-sharing tetrahedra. With a nearest-neighbor antiferromagnetic (AFM) exchange interaction on three-fold rings, this system is completely frustrated[5,9], and it has been shown that this frustration should prevent magnetic ordering down to zero temperature[10]. In spite of this, the magnetic spinels generally do show magnetic ordering, though at temperatures much lower than the scale set by the exchange interaction (this ratio is called the "frustration factor"). The ordering results from the fact that the spins couple to other degrees of freedom, such as orbital ordering and lattice distortion, to relieve the frustration and pick out a particular lowest-free-energy equilibrium state. In each case, the observed ordering depends on the details of the coupling and energetics of the individual system.

In particular, the chromium spinels ACr$_2$O$_4$ (Cr^{+3} with S=$\frac{3}{2}$; A=Cd, Zn and Hg) exhibit first-order phase transitions from a paramagnetic cubic structure to a low-temperature magnetically-ordered tetragonal phase at 7.8, 12.7 and 12.5 K respectively[5,6]. ZnCr$_2$O$_4$ has a Curie-Weiss temperature | Θ |$\approx$ 390 K, while the phase transition occurs at T_N=12.7K (the frustration factor is $\approx$ 31), whereas CdCr$_2$O$_4$ has a Curie-Weiss temperature

| Θ |$\approx$ 88 K and the phase transition occurs at T_N =7.8 K. The lifting of frustration is achieved via the tetragonal distortion, the details of which depend on the A cation. In the case of ZnCr$_2$O$_4$, the phase transition involves a tetragonal contraction along the c-axis ($c < a$) and commensurate Neél ordering with multiple wave-vectors[3]. In the case of CdCr$_2$O$_4$, however, the transition involves a tetragonal elongation along the c-axis ($c > a$) and an incommensurate (IC) Neél ordering with wave vector $\mathbf{k} = (0, \delta, 1)$. The difference in the ordered state for these two otherwise very similar systems reflects subtle differences in the magnetic interactions and in the coupling of the spins to the lattice distortions, which determine the delicate balance between the lattice energy cost for the distortion and the magnetic energy gain due to the spin ordering.

First-principles calculations for these systems can provide valuable information about the spin-lattice coupling, by which we mean the dependence of the energy as a function of atomic displacements on magnetic ordering. Specifically, with first-principles methods we can compute the pattern of forces on atoms and the distortions induced by a particular magnetic ordering[11,12] as well as the spin-phonon coupling, by which we mean the dependence of phonon frequencies in a given structure on magnetic ordering. A theory based on Dzyaloshinskii-Moriya interactions was proposed to explain the static spin-lattice coupling in CdCr$_2$O$_4$[13,14]. The effect of magnetic ordering on zone-center phonons has been well studied both from first principles and in experiment[13,15–17]. Recently, experimental observation has been extended to the full phonon dispersion relation of CdCr$_2$O$_4$[18] and its changes through the phase transition. First principles calculations of the phonon dispersion can be used to interpret these observations, in particular to resolve the
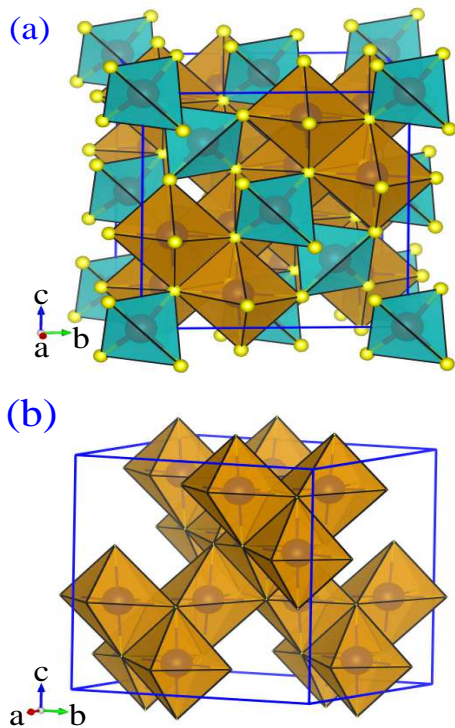
FIG. 1. (Color online) (a) The crystal structure of $CdCr_2O_4$ consisting of Cr centred octahedra and Cd centred tetrahedra. The O atoms are shown in yellow. (b) The Cr centred octahedra form a three dimensional pyrochlore sublattice.

question of whether the changes in the phonons through the transition primarily arise from the change in magnetic ordering, through spin-phonon coupling, or from the change in crystal structure.

In this paper, we use first principles calculations to investigate the effects of magnetic ordering on the minimum-energy structure and on the full phonon dispersion relation of $CdCr_2O_4$. By comparing ferromagnetic ordering with a layered antiferromagnetic ordering, we determine the lattice distortion induced by the lower-symmetry antiferromagnetic ordering, estimate the magnitude of spin-phonon coupling, and extract phonon frequencies for the paramagnetic phase. We find that the computed phonon dispersion for the cubic paramagnetic phase compares well with the experimental results. While the spin-phonon couplings are large for modes which involve displacement of the Cr atoms, there are no unstable modes at any point in the Brillouin zone for either of the magnetic orderings considered, suggesting that the symmetry breaking at the phase transition is not produced by a magnetically-induced phonon instability. Rather, the symmetry breaking is in the magnetic ordering, and the structural change through the transition is driven by the atomic forces and stresses induced by the magnetic order. Finally, by comparison of the phonon frequencies for structures with different magnetic

orderings and structural distortions, we find that this structural change is not the main factor in the changes in the phonon frequencies observed through the transition, but rather that these changes are the result, via the spin-phonon coupling, of the magnetic ordering at the transition.

II. METHOD

We performed density functional theory calculations using the generalized gradient approximation (GGA) with the Perdew-Burke-Ernzerhof (PBE) parameterization for the exchange correlation functional as implemented in the Quantum Espresso simulation package[19]. Interaction between valence electrons and ionic cores is treated using ultrasoft[20] pseudopotentials. The pseudopotentials we used include 12 valence electrons for Cd ($4d^{10}, 5s^2$), 14 for Cr ($3s^2, 3p^6, 3d^5, 4s^1$), and 6 for O ($3s^2, 2p^4$). We used a plane wave cutoff of 30 Ryd and $6 \times 6 \times 6$ Monkhorst Pack[21] k-point mesh for the Brillouin zone (BZ) integration. All calculations are performed for collinear spins without spin-orbit coupling. The optimization of atomic positions was carried through the minimization of energy using Hellman-Feynman forces acting on atoms with the Broyden-Flecher-Goldfarb-Shanno (BFGS) scheme.

As discussed in the Introduction, the observed magnetic ordering in $CdCr_2O_4$ is quite complex, and direct first-principles calculation of the full phonon dispersion for this phase would requires too large a supercell to be computationally practicable. However, calculations for magnetic orderings with smaller supercells can give us the information about the magnitude of spin-lattice couplings that we need to determine whether the spin-phonon coupling is large enough to produce the observed changes in the phonon dispersion through the magnetic transition, and to what extent these changes are the result of the change in crystal structure. Here, we consider two magnetic orderings: ferromagnetic (FM) and antiferromagnetic (AFM) ordering of the spins of the four Cr atoms in the fourteen-atom primitive unit cell. In the cubic unit cell, all arrangements of two up and two down spins on the four Cr atoms for the AFM ordering are symmetry equivalent, giving an arrangement in which layers of up and down spins alternate along a cartesian axis (chosen here to be the z axis).

The phonon frequencies and eigenvectors were computed using the linear response method for cubic ($Fd\bar{3}m$) and tetragonal ($I4_1/amd$) structures with the FM and AFM orderings. We computed interatomic force constants (IFCs) in reciprocal space on a $2 \times 2 \times 2$ q grid. The full phonon dispersion was obtained by the interpolation method[22], in which the asymptotic long-range dipole-dipole form of the interatomic force constants is determined by calculated values of the Born effective charges and dielectric constant. The latter were obtained using VASP[23,24], as this capability is not currently avail-

TABLE I. The calculated Born effective charge and dielectric constant tensors of $CdCr_2O_4$ for the FM and AFM orderings in the cubic structure.

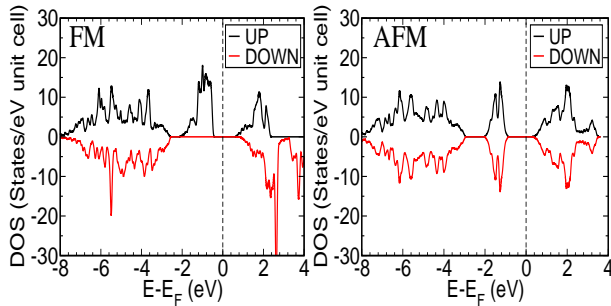| AFM				FM			
Cd	Cr	O	ϵ_∞	Cd	Cr	O	ϵ_∞
2.35 0.00 0.00	3.02 0.92 0.92	-2.10 0.11 0.11	6.11 0.00 0.00	2.37 0.00 0.00	3.15 0.81 0.81	-2.17 0.10 0.10	6.53 0.00 0.00
0.00 2.37 0.00	0.88 3.11 0.76	0.14 -2.15 0.06	0.00 6.32 0.00	0.00 2.37 0.00	0.81 3.15 0.81	0.10 -2.17 0.10	0.00 6.53 0.00
0.00 0.00 2.37	0.88 0.76 3.11	0.14 0.06 -2.15	0.00 0.00 6.32	0.00 0.00 2.37	0.81 0.81 3.15	0.10 0.10 -2.17	0.00 0.00 6.53

FIG. 2. (Color online) Electronic density of states of $CdCr_2O_4$ for the FM and AFM orderings in the cubic structure.
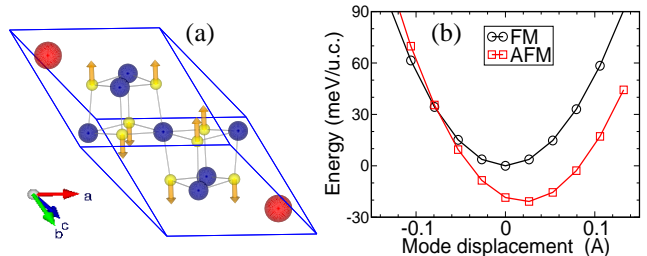

FIG. 3. (Color online)(a) The force pattern induced by the AFM ordering in the FM relaxed structure in a primitive unit cell. The Cd atoms are in red, Cr are in blue and O are in yellow. (b) The energy as a function of amplitude for the FM and AFM orderings in the cubic structure.

able for spin-polarized systems in Quantum Espresso, and the values are given in Table I. In these calculations we used the same GGA functional and other computational parameters given above. We used experimental lattice constants[7] (cubic a_0=8.588 Å) for the calculation of the phonon dispersion to facilitate comparison with the experimental phonon dispersion.

To obtain the phonon dispersion for the PM ordering, we averaged the interatomic force constant matrices (IFCs) obtained for the FM and AFM orderings so that each Cr-Cr bond has an equal fraction of aligned and anti-aligned spins. As we will see in more detail in Section III.C, this is an approximation that relies on two assumptions: (1) that the time scale for phonons is much longer than for spin fluctuations, and (2) that the spins in the paramagnetic phase are uncorrelated; these assumptions correspond to the high-temperature limit. The averaging procedure required generation of IFCs for the three different AFM configurations related by three-fold rotation around [111]. In the cubic structure, the IFCs can be obtained by transformation of the IFCs obtained for calculation of a single AFM configuration; in the tetragonal structure the IFCs have to be separately calculated for two AFM configurations, one of which is related to the third by symmetry. A given bond has spins aligned in one of these configurations and spins antialigned in two. Averaging with equal weight over these three configurations and the FM configuration results in an equal fraction of aligned and antialigned spins for each bond. The PM IFCs can equivalently be obtained using the parameterization discussed in section III (C). The Born effective charges for the PM ordering are obtained by the same averaging over the four configurations as for the IFCs.

III. RESULTS AND DISCUSSION

A. Energetics of different magnetic orderings and structures

We optimized the crystal structures with the FM and AFM orderings. The lowest-energy structure for FM ordering is cubic (a=8.667 Å) whereas for the AFM ordering it is tetragonal (a=b=8.634 Å and c=8.694 Å). The computed values are in very good agreement with the experimental lattice constant[7,15] for the cubic phase a=8.588 Å and (c-a)/a=0.5×10^{-3} for the tetragonal phase (noting, however, that the magnetic ordering is not the same as in the experimental phase), with the expected overestimation associated with the use of the GGA functional. The computed internal structural parameter for the atomic positions of O atoms in the spinels is u=0.2689 for the FM ordering. The O atoms in the optimized AFM occupy the Wyckoff position 16h (0,0.210,0.391) of the space group $I4_1/amd$. The calculated magnetic moment for the Cr ion is S=$\frac{3}{2}$, as expected for a high-spin d^3 system. The calculated electronic band gap at the experimental lattice constant is 1.1 eV in the FM structure and 1.3 eV in the AFM structure (see Fig. 2).

The total energy calculations of the FM and AFM orderings in the cubic structure at the experimental lattice constant show that AFM ordering has energy lower than that of FM ordering by 9.26 meV/f.u. The change in total energy with spin orderings can be used to estimate the nearest-neighbor exchange interaction coefficient **J** using the classical Heisenberg model: $E_{spin} =$

TABLE II. The IR active phonon frequencies (in cm^{-1}) at q=(000) for the FM, AFM and PM orderings in the cubic and tetragonal structures. The frequencies shown in bold are doublet modes.

Cubic			Tetragonal			
FM	AFM	PM	FM	AFM(x)	AFM(z)	PM
150	**127**,151	145	**149**,152	**128**,149	**126**,152	**144**,146
368	**321**,370	354	**364**,366	**319**,366	**317**,367	**350**,352
445	**439**,444	445	**441**,443	**435**,442	**434**,438	**441**,443
586	**580**,594	585	**579**,580	**573**,587	**572**,588	**578**,579

TABLE III. The splitting of doublet modes at L point q=($\frac{1}{2}$,$\frac{1}{2}$,$\frac{1}{2}$) of FM, AFM and PM orderings in the cubic and tetragonal structures. The frequencies are in cm^{-1}.

Cubic			Tetragonal			
FM	AFM	PM	FM	AFM(x)	AFM(z)	PM
166	148,162	162	165,166	148,160	149,162	161,162
273	253,267	267	271,272	252,267	245,267	265,266
353	306,330	339	349,350	304,329	306,329	336,337
443	444,453	445	439,440	436,446	439,447	439,440

$E_0 - 2\mathbf{J}\sum_{\langle ij \rangle} \mathbf{S}_i.\mathbf{S}_j$. In spinels, magnetic atom (Cr) has six first nearest-neighbor sites ($z = 6$) and the energies for the FM and AFM orderings are given as: $E_{FM} = E_0 - 24\mathbf{J}S^2$ and $E_{AFM} = E_0 + 8\mathbf{J}S^2$ respectively. We estimate $J = -0.26$ meV for CdCr$_2$O$_4$ which compares well with the experimental value (3 $k_B| \Theta |$ $/2zS(S+1) = -0.38$ meV) and is an order of magnitude smaller than that of ZnCr$_2$O$_4$[25].

The change in the magnetic ordering from FM to AFM ordering induces tetragonal stresses and a tetragonal force pattern in the optimized FM cubic structure. The displacement of atoms according to the forces induced due to AFM ordering lowers the energy (by 12.9 meV/f.u.) relative to the FM phase, as shown in Fig.3, leading to a tetragonal symmetry with space group $I4_1/amd$. The relaxation of the stresses induced by AFM ordering further lowers the energy without breaking additional symmetry. Similarly, the symmetry breaking in the magnetic ordering at the observed phase transition results in a low temperature tetragonal phase.

B. Phonons

To separate the effects of magnetic ordering and structural change on the phonon frequencies and eigenvectors, we performed first-principles calculations of the phonon dispersion relation for four configurations: (1) cubic (a=8.588 $\mathring{A}$, u=0.2686) with FM ordering; (2) cubic with AFM ordering; (3) tetragonal (a=b=8.588 $\mathring{A}$, c=8.649 $\mathring{A}$, O at 16h(0,0.213,0.394)) with FM ordering; and (4) tetragonal with AFM ordering. In the tetragonal structure, atoms Cd, Cr and O occupy the Wyckoff positions 4a, 8h and 16h of space group $I4_1/amd$ respectively. From these, we extract the phonon dispersion for the PM ordering for both the cubic and tetragonal structures by the averaging procedure described above.

First, we consider the results for the phonons in the cubic structure for the FM and AFM orderings, which highlights the spin-phonon coupling in this system. The frequencies of the IR-active phonon modes at $\vec{q} = 0$ are reported in Table II. The 150 cm^{-1} triplet mode of cubic FM splits into a doublet at 127 cm^{-1} and a singlet at 151 cm^{-1} in the cubic AFM phase. The triplet mode at 368 cm^{-1} in the cubic FM shows the largest splitting, consis-
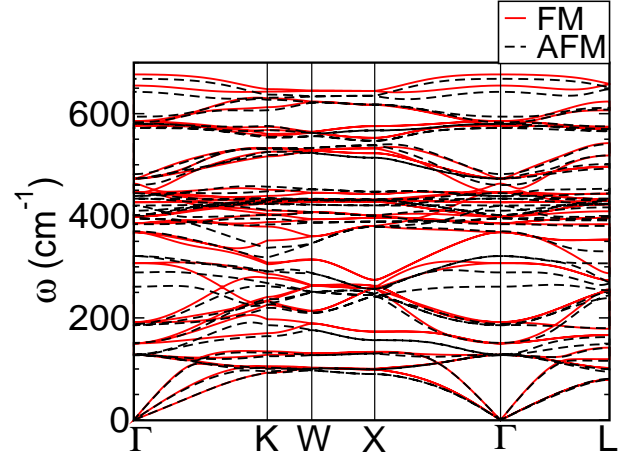

FIG. 4. (Color online) A comparison of the cubic FM and AFM phonon dispersion relations.

tent with the experimental observation that the triplet modes at 354 cm^{-1} show the largest splitting. However, we find that the doublet is 49 cm^{-1} below the singlet, the reverse of the observed level order. The suggestion that is due to the fact that the AFM order we consider is not the ground state magnetic ordering is supported by recent first principles calculations[26] for the $\vec{q} = 0$ modes with the observed ground-state spin order, which do give the correct splitting and level order. The other IR-active modes at 445 and 586 cm^{-1} show relatively weak splitting with the change in the magnetic ordering from FM to AFM.

Next, we consider the splitting of doublet modes at L point in the BZ (q=($\frac{1}{2}$,$\frac{1}{2}$,$\frac{1}{2}$)) with change in magnetic ordering from FM to AFM. In Table III, we present frequencies of E_u modes that have large splittings. The doublet mode at 353 cm^{-1} in the cubic FM shows the largest splitting (24 cm^{-1}) in the cubic AFM. The modes at 166 cm^{-1} and 273 cm^{-1} in the cubic FM show splitting of 14 cm^{-1} in the cubic AFM (see Table III). Other modes also show moderate splittings in the range of 5-10 cm^{-1}.

Phonon dispersion relations throughout the Brillouin zone for the FM and AFM orderings provide information about the role of spins in the short range interactions. In Fig 4, we show phonon dispersion relations for the FM and AFM orderings in cubic structures (see Fig 4). We do not find any unstable modes throughout the BZ for
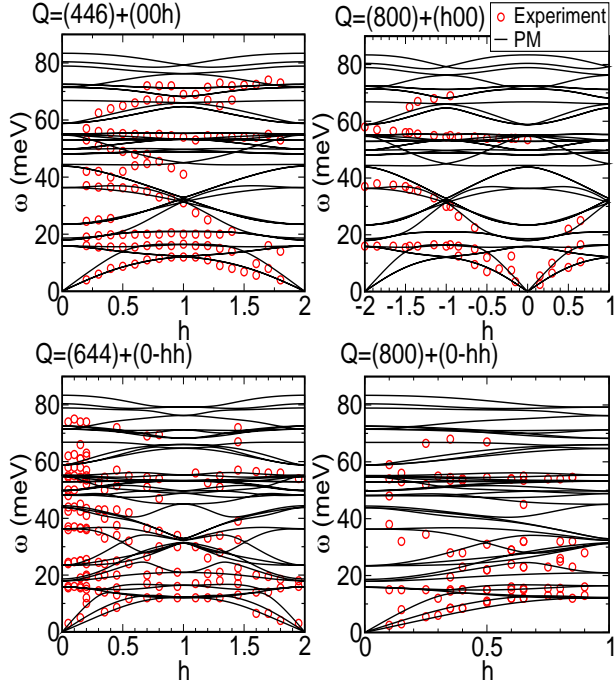
FIG. 5. (Color online) A comparison of the calculated phonon dispersion relation for the cubic PM with the experimental phonon dispersion obtained at 10K[18].
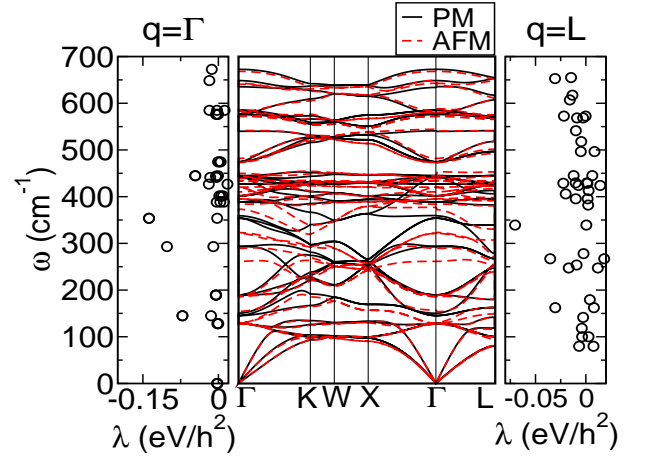
FIG. 6. (Color online) Comparison of the computed phonon dispersion relations of the PM and AFM phases, with the strengths of spin-phonon coupling at $q = 0$ and q=$(\frac{1}{2}, \frac{1}{2}, \frac{1}{2})$ plotted in the two side panels.

either magnetic ordering. Analysis of the eigen vectors of the phonon modes shows that low frequency modes up to 160 cm^{-1} involve displacement of Cd atoms, modes with frequency range 161-500 cm^{-1} involve displacements of Cr and O atoms and higher frequencies modes involve displacement of O atoms. The modes which involves both Cr and O displacements have larger spin-phonon coupling.

In order to compare the computed phonon dispersion with the experiment, we estimate the PM phonon dispersion relation using the averaging procedure as described above. The computed zone center frequencies and L point frequencies for IR active modes are shown in Tables II and III. We present our first-principles phonon dispersion relation for the cubic PM phase in Fig. 5, plotted with the experimental results obtained using inelastic x-ray scattering at 10K[18]. We find a close correspondence between our first-principles calculations and the experimentally determined frequencies, noting that not all the branches are observed in the experimental determination. This suggests that the first-principles results provide a useful framework for interpreting the experimental phonon observations.

C. Spin-phonon coupling

From the difference between the FM and AFM results, we can extract a quantitative parametrization of the spin-phonon coupling. Following Ref. 25, the real-

space IFCs for different magnetic orderings can be expanded around the paramagnetic real-space IFCs using the second derivative of the exchange interaction *w.r.t.* small atomic displacements:

$$\tilde{C}_{\vec{R}i\alpha\vec{R}'j\beta} = C_{\vec{R}i\alpha\vec{R}'j\beta} - \sum_{mn} \mathcal{J}''_{\vec{R}i\alpha\vec{R}j\beta;mn}\langle \vec{S}_m \cdot \vec{S}_n\rangle, \quad (1)$$

where $\tilde{C}$ is the matrix of IFCs for a particular magnetic ordering, C is the matrix of IFCs for the paramagnetic phase, $\mathcal{J}''$ is the second derivative of the exchange interaction J *w.r.t.* atomic displacements, the sums over m and n run over the magnetic atoms in the system, and the indices $\vec{R}$, i and α refer to the displacement of the atom i in the unit cell labelled by lattice vector $\vec{R}$ along Cartesian direction α. Here, we explicitly see the approximations mentioned in Section II above. Thermal averaging of the spin configuration is based on the assumption that the time scale for phonons is much longer than for spin fluctuations, and we take $\langle \vec{S}_m \cdot \vec{S}_n\rangle = 0$ in the paramagnetic phase based on the assumption that the spins in the paramagnetic phase are uncorrelated.

Information about the matrix $\mathcal{J}''$ can be obtained using the reciprocal-space matrices of IFCs for different magnetic orderings. Here, we consider only magnetic orderings with the periodicity of the spinel structure unit cell (PM, FM, AFM). Eq.1 for the FM and AFM orderings can be written as

$$\tilde{C}^{FM} = C - 2\mathcal{J}''_{yz}S^2 - 2\mathcal{J}''_{xz}S^2 - 2\mathcal{J}''_{xy}S^2$$
$$\tilde{C}^{AFM_x} = C - 2\mathcal{J}''_{yz}S^2 + 2\mathcal{J}''_{xz}S^2 + 2\mathcal{J}''_{xy}S^2$$
$$\tilde{C}^{AFM_y} = C + 2\mathcal{J}''_{yz}S^2 - 2\mathcal{J}''_{xz}S^2 + 2\mathcal{J}''_{xy}S^2$$
$$\tilde{C}^{AFM_z} = C + 2\mathcal{J}''_{yz}S^2 + 2\mathcal{J}''_{xz}S^2 - 2\mathcal{J}''_{xy}S^2$$

where $\tilde{C}$, C and $J^{''}$ depend on $\vec{q}$ but explicit dependence on $\vec{q}$ has been suppressed in above equations. The $\tilde{C}^{AFM_x}$, $\tilde{C}^{AFM_y}$ and $\tilde{C}^{AFM_z}$ are the IFCs for AFM with layers of ferromagnetically aligned spin stacked along x, y and z respectively. Similarly, $\mathcal{J}^{''}_{yz}$, $\mathcal{J}^{''}_{xz}$ and $\mathcal{J}^{''}_{xy}$ are the sum of bonds connecting two magnetic atoms in yz, xz and xy planes respectively. We suppressed the explicit dependence of C and $J^{''}$ on the $\vec{q}$ in above equations. Here, we consider nearest neighbor interaction between the magnetic atoms and ignore the further neighbor interactions for simplicity. The system of linear equations can be solved to obtain $\mathcal{J}^{''}_{yz}$, $\mathcal{J}^{''}_{xz}$, and $\mathcal{J}^{''}_{xy}$.

The strength of spin-phonon coupling parameter λ_i for any phonon mode i ($|\psi_i(q)\rangle$) can be estimated from the interaction matrices $\mathcal{J}^{''}_{yz}$,$\mathcal{J}^{''}_{xz}$ and $\mathcal{J}^{''}_{xy}$. The frequency shift and splitting of each mode of PM due to AFM_z ordering is given as,

$$\lambda_i = \langle\psi_i(q)|(\mathcal{J}^{''}_{yz} + \mathcal{J}^{''}_{xz} - \mathcal{J}^{''}_{xy})(q)|\psi_i(q)\rangle. \quad (2)$$

We calculated the strength of spin-phonon coupling for all the phonon modes of the PM ordering in the cubic structure of $CdCr_2O_4$ at q= (000) and q=$(\frac{1}{2},\frac{1}{2},\frac{1}{2})$. The unit of λ is eV/h^2, where h is the Planck constant. In Fig.6, we quantitatively show the strength of spin-phonon coupling for each mode, which overall agrees very well with the shifts and splittings of the AFM phonon modes from the PM modes. The largest spin phonon coupling at $q = 0$ is for the IR active mode at $354 \ cm^{-1}$, which is consistent with the large splitting observed in experiments[15,18] and in the first principles results as discussed above. The doublet E_u mode at $293 \ cm^{-1}$ in the PM also shows a large spin-phonon coupling. The other IR active modes which show large spin-phonon coupling are the modes at $145 \ cm^{-1}$ and $445 \ cm^{-1}$ (see Fig.6). At q=$(\frac{1}{2},\frac{1}{2},\frac{1}{2})$, the values are smaller than at q= (000). The E_u mode at $339 \ cm^{-1}$ shows large spin-phonon coupling. The other modes which have large spin-phonon coupling are E_u modes at $162 \ cm^{-1}$ and $267 \ cm^{-1}$ (see Fig.6). Examination of the eigenvectors show that those modes which involve displacement of Cr and O atoms together have the largest spin-phonon coupling.

D. Relative effects of magnetic ordering and tetragonal distortion on phonon dispersion

As discussed in the Introduction, $CdCr_2O_4$ undergoes a phase transition from the cubic PM phase to a tetragonal magnetically-ordered phase at low temperature. To interpret the changes in phonon frequencies through the transition, we computed full phonon dispersion relations of both the cubic and the tetragonal structures with the PM and AFM orderings, shown together in Fig.7. Although the AFM ordering we have considered in this work is not the observed ground state magnetic ordering, the magnitude of the shifts in the phonon frequencies between the PM and AFM orderings should be comparable
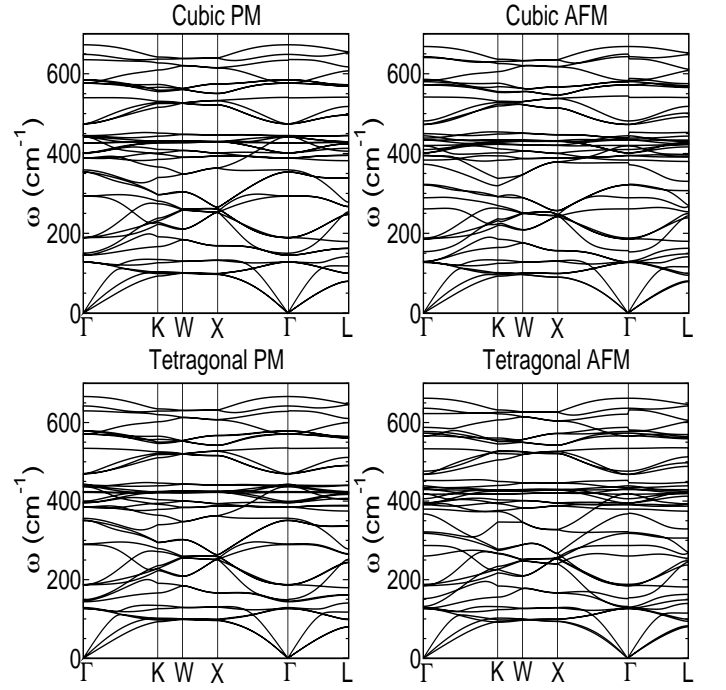

FIG. 7. Effect of magnetic ordering and structural distortion on the phonon dispersion relations.

to those between the PM and observed ground-state magnetic ordering, and this analysis allows us to separate the effects of the magnetic ordering and the structural distortion on the phonons, as already discussed above.

The comparison of the phonons in the cubic structure for PM and FM ordering has been presented above in Tables II and III, showing the splitting of IR active modes with the spin ordering and tetragonal distortion at the zone center ($\vec{q} = 0$) and L point in the BZ. The differences for PM and FM ordering in the tetragonal structure are similar, as further seen in Tables II and III. Detailed analysis of the IFCs of the PM and AFM orderings shows that the changes in the phonon dispersion relations for the two structures are mainly from the changes in the IFCs between Cr-Cr and Cr-O atoms.

The effect of tetragonal distortion on the phonon can be seen by comparing the cubic PM phonon dispersion to that of the tetragonal PM phase and the cubic AFM phonon dispersion to the tetragonal AFM phase in Fig.7 and in Tables II and III. We find that the differences due to tetragonal distortion are much smaller than the changes induced by magnetic ordering. The largest change in phonon frequencies at $q = 0$ due to tetragonal distortion is $5 \ cm^{-1}$ for the mode at $585 \ cm^{-1}$.

IV. CONCLUSION

In summary, we have presented a first-principles study to investigate the effects of magnetic ordering on the minimum-energy structure and on the full

phonon dispersion relation of $CdCr_2O_4$, focusing on the changes through the coupled magnetic/structural transition which shows relief of the geometric frustration of the antiferromagnetic ordering on the pyrochlore lattice. The phonon dispersion for the cubic paramagnetic phase compares well with the experimental results. While the spin-phonon couplings are large for modes which involve displacement of the Cr atoms, there are no unstable modes at any point in the Brillouin zone for all the magnetic orderings considered, and thus we conclude that the phase transition is driven not by spin-phonon coupling but by the atomic forces and stresses induced by the AFM ordering. Finally, by comparison of the phonon frequencies for structures with different magnetic orderings and structural distortions, we find that the spin-phonon coupling, rather than the coupling of the phonons to the structural change, is the dominant factor in the observed changes of phonon frequencies through the phase transition.

[1] A. P. Ramirez, Ann. Rev. Mat. Sci. 24, 453 (1994).
[2] R. Moessner and A. P. Ramirez, Phys. Today 59, 24 (2006).
[3] S.-H. Lee, C. Broholm, T. H. Kim, W. Ratcliff and S-W. Cheong, Phys. Rev. Lett. 84, 3718 (2000).
[4] S.-H. Lee, C. Broholm, W. Ratcliff, G. Gasparovic, Q. Huang, T. H. Kim and S.-W. Cheong, Nature (London) 418 856 (2002).
[5] O. Tchernyshyov, R. Moessner, and S. L. Sondhi, Phys. Rev. Lett. 88, 067203 (2002).
[6] O. Tchernyshyov, R. Moessner, and S. L. Sondhi, Phys. Rev. B 66, 064403 (2002).
[7] J.-H. Chung, M. Matsuda, S.-H. Lee, K. Kakurai, H. Ueda, T. J. Sato, H. Takagi, K.-P. Hong and S. Park, Phys. Rev. Lett. 95, 247204 (2005).
[8] M. Matsuda, M. Takeda, M. Nakamura, K. Kakurai, A. Oosawa, E. Lelièvre-Berna, J.-H. Chung, H. Ueda, H. Takagi, and S-H Lee, Phys. Rev. B 75, 104415 (2007).
[9] R. Moessner and J. T. Chalker, Phys. Rev. Lett. 80, 2929 (1998).
[10] P. W. Anderson, Phys. Rev. 102, 1008 (1956).
[11] A. Filippetti and N. A. Hill, Phys. Rev. Lett. 85, 5166 (2000).
[12] K. M. Rabe, Annu. Rev. Condens. Matter Phys. 1, 211 (2010).
[13] G.-W. Chern, C. J. Fennie and O. Tchernyshyov, Phys. Rev. B 74, 060405(R) (2006).
[14] Subhro Bhattacharjee, S. Zherlitsyn, O. Chiatti, A. Sytcheva, J. Wosnitza, R. Moessner, M. E. Zhitomirsky, P. Lemmens, V. Tsurkan, and A. Loidl, Phys. Rev. B. 83, 184421 (2011).
[15] R. Valdes Aguilar, A. B. Sushkov, Y. J. Choi, S. W. Cheong and H. D. Drew, Phys. Rev. B 77, 092412 (2008).
[16] Ch. Kant, J. Deisenhofer, T. Rudolf, F. Mayr, F. Schrettle, A. Loidl, V. Gnezdilov, D. Wulferding, P. Lemmens, V. Tsurkan, Phys. Rev. B 80 214417 (2009).
[17] M. Matsuda, K. Ohoyama, S. Yoshii, H. Nojiri, P. Frings, F. Duc, B. Vignolle, G. L. J. A. Rikken, L.-P. Regnault, S.-H. Lee, H. Ueda, and Y. Ueda, Phys. Rev. Lett 104, 047201 (2010).
[18] J.-H. Kim, M. Matsuda, H. Ueda, Y. Ueda, J.-H. Chung, S. Tsutsu, A. Q. R. Baron, and S.-H. Lee, J. Phys. Soc. Jpn. 80 073603 (2011).
[19] P. Giannozzi, S. Baroni, N. Bonini, M. Calandra, R. Car, C. Cavazzoni, D. Ceresoli, G. L. Chiarotti, M. Cococcioni, I. Dabo, A. Dal Corso, S. d. Gironcoli, S. Fabris, G. Fratesi, R. Gebauer, U. Gerstmann, C. Gougoussis, A. Kokalj, M. Lazzeri, L. Martin-Samos, N. Marzari, F. Mauri, R. Mazzarello, S. Paolini, A. Pasquarello, L. Paulatto, C. Sbraccia, S. Scandolo, G. Sclauzero, A. P Seitsonen, A. Smogunov, P. Umari and R. M. Wentzcovitch, J. Phys. Condens. Matter 21, 395502 (2009).
[20] D. Vanderbilt, Phys. Rev. B 41, 7892 (1990).
[21] J. D. Pack and H. J. Monkhorst, Phys. Rev. B 13, 5188 (1976); ibid Phys. Rev. B 16, 1748 (1977).
[22] X. Gonze, D. C. Allan and M. P. Teter, Phys. Rev. Lett. 68, 3603 (1992).
[23] G. Kresse and J. Hafner, Phys. Rev. B 49, 14251 (1994).
[24] G. Kresse and J. Furthmüller, Phys. Rev. B 54, 11169 (1996).
[25] C. J. Fennie and K. M. Rabe, Phys. Rev. Lett. 96, 205505 (2006).
[26] T. Birol, A. Wysocki and C. J. Fennie, in preparation.